J. Plasma Physics (2006), *vol.* 72, *part* 3, *pp.* 285–308.
doi:10.1017/S0022377805004101 First published online 16 November 2005 Printed in the United Kingdom

Leaky and non-leaky kink oscillations of magnetic flux tubes

MICHAEL S. RUDERMAN[1] and BERNARD ROBERTS[2]

[1]Department of Applied Mathematics, University of Sheffield, Hicks Building, Hounsfield Road, Sheffield S3 7RH, UK
(m.s.ruderman@sheffield.ac.uk)

[2]School of Mathematics and Statistics, University of St Andrews, St Andrews, Fife KY16 9SS, UK

(Received 15 May 2005 and accepted 1 June 2005)

Abstract. We study the normal and leaky kink oscillations of a thin magnetic tube embedded in a surrounding magnetized plasma. We adopt the cold plasma (zero plasma β) approximation, appropriate for typical solar coronal conditions. Using the Laplace transform, we solve the initial value problem to determine the motions of the flux tube. The asymptotic description of this motion is determined by the properties of a dispersion function $D(\omega)$, an infinitely valued function of the complex frequency ω. Two cases arise. When the plasma density $\rho_{\rm i}$ inside the tube exceeds the density $\rho_{\rm e}$ of the surrounding plasma, the asymptotic behaviour is given by the normal mode that is associated with two zeros of $D(\omega)$. These zeros are real and symmetric with respect to the imaginary axis, and are situated on the principal sheet of the Riemann surface of $D(\omega)$. The asymptotics given by the normal mode is valid for times much longer than the period of tube oscillation, and is homogeneous with respect to the radial distance r. In the second case, where $\rho_{\rm i} < \rho_{\rm e}$, there are no zeros of $D(\omega)$ on the principal sheet. The asymptotics of the solution of the initial value problem is then given by a *leaky* mode of the tube kink oscillations. This mode is associated with two zeros of $D(\omega)$ on two different, non-principal, sheets of the Riemann surface of $D(\omega)$ attached to the principal sheet. The asymptotics given by the leaky mode is intermediate, i.e. valid for times much longer than the period of oscillations but smaller than (or of the order of) the damping time due to energy leakage. The asymptotics given by the leaky mode is inhomogeneous with respect to r. We also consider other solutions associated with the zeros of $D(\omega)$ on non-principal sheets, and argue that in the coronal loop case where $\rho_{\rm i} > \rho_{\rm e}$ these solutions have no physical meaning. In the opposite case, where $\rho_{\rm i} < \rho_{\rm e}$, only the two solutions associated with the two zeros of $D(\omega)$ lying on two different non-principal sheets attached to the principal sheet are physically meaningful; they determine the leaky mode. All other solutions of this type are devoid of physical meaning. On the basis of our results, we conclude that there is no radial wave energy leakage from a dense coronal loop oscillating in the kink mode; other mechanisms must be sought to explain the observed oscillation damping.

1. Introduction

Recent space observations of standing transverse oscillations of coronal loops (Aschwanden et al. 1999, 2002; Nakariakov et al. 1999; Schrijver and Brown 2000; Schrijver et al. 2002; Wang and Solanki 2004; Verwichte et al. 2005) obtained by the Transition Region and Coronal Explorer (TRACE) have considerably boosted interest in coronal waves and oscillations, and provided a serious challenge to theorists. Observational properties have been reviewed in Aschwanden (2004), Wang (2004) and Nakariakov and Verwichte (2005), and theoretical aspects are discussed in Roberts (2002, 2004), Roberts and Nakariakov (2003) and Nakariakov and Verwichte (2005). Loop oscillations are of particular importance because they provide diagnostic information about local coronal conditions, giving rise to a coronal seismology (Roberts et al. 1984; Nakariakov et al. 1999; Nakariakov and Ofman 2001).

The observations show that loops may oscillate in the kink mode, and do this with a frequency that is determined by conditions both inside and outside the loop. Specifically, for a thin cylindrical flux tube embedded in a magnetized plasma the kink oscillations have a frequency ω_k given by (see, for example, Edwin and Roberts 1983)

$$\omega_k = \left(\frac{2\rho_i}{\rho_\mathrm{i} + \rho_\mathrm{e}}\right)^{1/2} kV_\mathrm{Ai} \tag{1.1}$$

and so are determined by the plasma density ρ_i inside the tube and the density ρ_e in the environment of the tube, together with the longitudinal wave number k of the oscillation and the Alfvén speed V_Ai of the tube. However, the observations also reveal that loop oscillations are strongly damped. An understanding of this damping is important not only as a means of understanding coronal oscillations in general, but also because the damping itself provides diagnostic information about the corona that is additional to any information provided by the particular mode of oscillation. Various mechanisms of damping have been discussed (see, e.g., Roberts 2000) and continue to be under active investigation. Ruderman and Roberts (2002) suggested that the damping of loop oscillations is due to resonant absorption. This suggestion has been supported by Goossens et al. (2002) who analysed observations of 11 damped coronal loop oscillations and compared them with theoretical results; the conclusions are encouraging but not conclusive.

An alternative possibility for explaining wave damping is to examine the wave leakage that may result from an oscillating loop which sets up an outgoing wave radially propagating away from the loop. Recently, Cally (2003) suggested that at least part of the energy of a coronal loop oscillation can leak away in this way (see also Meerson et al. 1978; Spruit 1982; Cally 1986), though Cally (2003) concluded that generally the effect is not sufficient to explain the observations (see also Roberts 2000). More specifically, Cally (2003) argued that there exists a leaky kink mode of magnetic tube oscillations in the case where the plasma density inside a loop is larger than the density of the surrounding plasma, the circumstances typical of coronal conditions.

In this paper we study both leaky and non-leaky kink modes of a straight magnetic tube by solving the initial value problem. In particular, and in contradiction to Cally (2003), we show that there are *no* leaky modes when the plasma density inside the tube exceeds that of the surroundings. Thus, we argue that the observed damping of coronal kink oscillations cannot be explained, even in part, as a

consequence of radial leakage from an oscillating kink mode; some other mechanism must be sought.

Our paper is organized as follows. In the next section we formulate the problem, presenting the governing equations and the boundary and initial conditions. In Sec. 3 we obtain the solution of the initial value problem for kink oscillations, and then turn in Sec. 4 to a study of the asymptotic behaviour of solutions of the initial value problem. In Sec. 5 we discuss the meaning of solutions of the linear magnetohydrodynamic (MHD) equations that are associated with the zeros of the dispersion function on different sheets of the Riemann surface of this function. Finally, in Sec. 6, we summarize the results and present our conclusions.

2. Formulation

We consider oscillations of a magnetic tube in a cold (zero β) plasma. We use cylindrical coordinates r, φ, z. In equilibrium the magnetic field has constant magnitude B and it is in the z-direction. The magnetic field is frozen in dense plasmas at $z = 0, L$. The equilibrium plasma density, ρ, is equal to $\rho_{\rm i}$ inside the magnetic tube of radius R ($r < R$), and is equal to $\rho_{\rm e}$ outside the tube ($r > R$).

The motion of the perturbed plasma is described by the linear system of ideal MHD equations,

$$\frac{\partial u}{\partial t} = \frac{1}{\rho}\left(\frac{B}{\mu}\frac{\partial b_r}{\partial z} - \frac{\partial P}{\partial r}\right), \tag{2.1a}$$

$$\frac{\partial v}{\partial t} = \frac{1}{\rho}\left(\frac{B}{\mu}\frac{\partial b_\varphi}{\partial z} - \frac{1}{r}\frac{\partial P}{\partial \varphi}\right), \tag{2.1b}$$

$$\frac{\partial b_r}{\partial t} = B\frac{\partial u}{\partial z}, \quad \frac{\partial b_\varphi}{\partial t} = B\frac{\partial v}{\partial z}, \quad \nabla\cdot\boldsymbol{b} = 0, \tag{2.1c}$$

$$\frac{\partial P}{\partial t} = -\frac{\rho V_{\rm A}^2}{r}\left[\frac{\partial (ru)}{\partial r} + \frac{\partial v}{\partial \varphi}\right]. \tag{2.1d}$$

Here $\boldsymbol{v} = (u, v, 0)$ is the velocity, $\boldsymbol{b} = (b_r, b_\varphi, b_z)$ is the perturbation of the magnetic field and $P = Bb_z/\mu$ is the perturbation of the magnetic pressure; $V_{\rm A} = B(\mu\rho)^{-1/2}$ is the Alfvén speed, with μ being the magnetic permeability of empty space. These equations were discussed in Ruderman and Roberts (2002).

We assume that the dense plasmas in the regions $z < 0$ and $z > L$ are immovable. Then it follows from the frozen-in condition that

$$u = v = 0 \quad \text{at } z = 0, L. \tag{2.2}$$

Boundary condition (2.2) coupled with (2.1d) implies that

$$P = 0 \quad \text{at } z = 0, L. \tag{2.3}$$

Differentiating (2.1d) with respect to time and using (2.1a), (2.1b) and the third equation in (2.1c), we obtain that P satisfies the wave equation

$$\frac{\partial^2 P}{\partial t^2} = V_{\rm A}^2 \nabla^2 P. \tag{2.4}$$

https://doi.org/10.1017/S0022377805004101 Published online by Cambridge University Press

Using the first equation in (2.1c), we arrive at

$$\frac{\partial^2 u}{\partial t^2} - V_{\rm A}^2 \frac{\partial^2 u}{\partial z^2} = -\frac{1}{\rho}\frac{\partial^2 P}{\partial t \partial r}. \tag{2.5}$$

The magnetic pressure perturbation P and the radial velocity u have to be continuous at the tube boundary (see, for example, Edwin and Roberts 1983), so that

$$[P] = 0, \quad [u] = 0 \quad \text{at } r = R, \tag{2.6}$$

where the square brackets indicate the jump of a quantity across the tube boundary.

In what follows we consider only the kink mode of the tube oscillations and take perturbations of all quantities to be proportional to $e^{i\varphi}$. In addition, we consider only the fundamental mode in the z-direction and, in accordance with the boundary conditions (2.2) and (2.3), take u and P to be proportional to $\sin(\pi z/L)$. Then (2.4) and (2.5) reduce to

$$\frac{\partial^2 P}{\partial t^2} = V_{\rm A}^2 \left(\frac{1}{r}\frac{\partial}{\partial r} r \frac{\partial P}{\partial r} - \frac{P}{r^2} \right) - \omega_{\rm A}^2 P, \tag{2.7}$$

$$\frac{\partial^2 u}{\partial t^2} + \omega_{\rm A}^2 u = -\frac{1}{\rho}\frac{\partial^2 P}{\partial t \partial r}, \tag{2.8}$$

where $\omega_{\rm A} = \pi V_{\rm A}/L$. Our analysis remains applicable to an overtone if we regard L as the distance between successive nodes along the loop.

To complete the formulation of the problem we have to specify initial conditions at $t = 0$ as

$$P = P_0, \quad \frac{\partial P}{\partial t} = \dot{P}_0, \quad u = u_0, \quad \frac{\partial u}{\partial t} = \dot{u}_0. \tag{2.9}$$

In what follows we assume that, at the initial moment of time, the plasma is perturbed only in a finite region, i.e. all perturbations are identically zero for $r > r_0 > R$.

The system of equations (2.7) and (2.8) with the boundary conditions (2.6) and the initial conditions (2.9) will be used in what follows to study the kink oscillations of the magnetic tube.

3. Solution of the initial value problem

To solve the initial value problem we introduce the Laplace transform

$$\hat{f}(\omega) = \int_0^\infty f(t) e^{i\omega t}\, dt. \tag{3.1}$$

Applying this transform to equations (2.7) and (2.8), we obtain

$$\frac{d^2 \hat{P}}{dr^2} + \frac{1}{r}\frac{d\hat{P}}{dr} + \left(\Lambda^2 - \frac{1}{r^2} \right) \hat{P} = \frac{i\omega P_0 - \dot{P}_0}{V_{\rm A}^2} \equiv F, \tag{3.2}$$

$$\rho\left(\omega^2 - \omega_{\rm A}^2\right)\hat{u} = -i\omega \frac{d\hat{P}}{dr} + i\omega u_0 - \dot{u}_0 - \frac{1}{\rho}\frac{dP_0}{dr}, \tag{3.3}$$

where

$$\Lambda^2 = \frac{\omega^2 - \omega_{\rm A}^2}{V_{\rm A}^2}. \tag{3.4}$$

https://doi.org/10.1017/S0022377805004101 Published online by Cambridge University Press

For simplicity, we take

$$u_0 = 0, \quad \dot{u}_0 + \frac{1}{\rho}\frac{dP_0}{dr} = 0. \tag{3.5}$$

Then, using (3.3), we rewrite the boundary conditions (2.6) as

$$[\hat{P}] = 0, \quad \left[\frac{1}{\rho(\omega^2 - \omega_{\mathrm{A}}^2)}\frac{d\hat{P}}{dr}\right] = 0. \tag{3.6}$$

Now we have to obtain the solution of (3.2) satisfying the boundary conditions (3.6) and the additional condition that P is regular at $r = 0$ and vanishes as $r \to \infty$. First we find the solution for ω in the upper part of the complex ω-plane, i.e. when $\Im(\omega) > 0$, where $\Im$ indicates the imaginary part of a quantity. Then we consider its analytical continuation in the lower part of the complex ω-plane. We will solve the problem separately inside and outside the tube.

3.1. Solution inside the tube

Let us introduce the notation $A(t) = P(t, R)$ and make the variable substitution

$$Q_{\mathrm{i}} = \hat{P} - \hat{A}\frac{I_1(\pi r/L)}{I_1(\pi R/L)}, \tag{3.7}$$

where $I_1(z)$ is the modified Bessel function of the first kind. Substituting (3.7) in (3.2) we obtain

$$\frac{d^2Q_{\mathrm{i}}}{dr^2} + \frac{1}{r}\frac{dQ_{\mathrm{i}}}{dr} + \left(\Lambda_{\mathrm{i}}^2 - \frac{1}{r^2}\right)Q_{\mathrm{i}} = F_{\mathrm{i}} - \frac{\omega^2 I_1(\pi r/L)}{V_{\mathrm{Ai}}^2 I_1(\pi R/L)}\hat{A}, \tag{3.8}$$

where, and in what follows, the subscripts 'i' and 'e' indicate that a quantity is calculated inside and outside the tube, respectively. The function Q_{i} satisfies the boundary conditions

$$Q_{\mathrm{i}}(r) \text{ is regular at } r = 0, \quad Q_{\mathrm{i}}(r = R) = 0. \tag{3.9}$$

The Green function of (3.8), $G_{\mathrm{i}}(r, s; \omega)$, considered as a function of r, has to satisfy the homogeneous equation (3.8) for $r \neq s$, the boundary conditions (3.9), to be continuous at $r = s$, and its derivative with respect to r has to have a jump equal to unity at $r = s$:

$$\lim_{\varepsilon \to +0}\left(\left.\frac{dG_{\mathrm{i}}}{dr}\right|_{r=s+\varepsilon} - \left.\frac{dG_{\mathrm{i}}}{dr}\right|_{r=s-\varepsilon}\right) = 1. \tag{3.10}$$

To construct the Green function we need two linearly independent solutions of the homogeneous equation (3.8), one satisfying the first boundary condition in (3.9), and the other satisfying the second boundary condition in (3.9). The first solution can be taken to be equal to $J_1(\Lambda_{\mathrm{i}} r)$, where $J_1(z)$ is the Bessel function of the first kind. To obtain the second solution we use the Hankel function of the first kind $H_1^{(1)}(z)$. Then the second solution is equal to

$$J_1(\Lambda_{\mathrm{i}} r)H_1^{(1)}(\Lambda_{\mathrm{i}} R) - J_1(\Lambda_{\mathrm{i}} R)H_1^{(1)}(\Lambda_{\mathrm{i}} r).$$

Using the relation $H_1^{(1)}(z) = J_1(z) + iY_1(z)$, where $Y_1(z)$ is the Bessel function of the second kind, and the identity (Abramowitz and Stegun 1964)

$$J_1(z)Y_1'(z) - J_1'(z)Y_1(z) = \frac{2}{\pi z}, \tag{3.11}$$

https://doi.org/10.1017/S0022377805004101 Published online by Cambridge University Press

where a prime indicates the derivative, we eventually arrive at

$$G_{\rm i}(r,s;\omega)=\frac{i\pi s}{2J_1(\Lambda_{\rm i}R)}\big\{\Theta(s-r)J_1(\Lambda_{\rm i}r)\big[J_1(\Lambda_{\rm i}s)H_1^{(1)}(\Lambda_{\rm i}R)-J_1(\Lambda_{\rm i}R)H_1^{(1)}(\Lambda_{\rm i}s)\big]$$
$$+\Theta(r-s)J_1(\Lambda_{\rm i}s)\big[J_1(\Lambda_{\rm i}r)H_1^{(1)}(\Lambda_{\rm i}R)-J_1(\Lambda_{\rm i}R)H_1^{(1)}(\Lambda_{\rm i}r)\big]\big\}, \quad (3.12)$$

where $\Theta(x)$ is the Heaviside function, $\Theta(x)=1$ for $x>0$ and $\Theta(x)=0$ for $x<0$. Then the solution of equation (3.8) satisfying the boundary conditions (3.9) is

$$Q_{\rm i}(r)=\int_0^R G_{\rm i}(r,s;\omega)\left\{F_{\rm i}(s)-\frac{\omega^2 I_1(\pi s/L)}{V_{\rm Ai}^2 I_1(\pi R/L)}\hat{A}\right\}ds. \quad (3.13)$$

3.2. Solution outside the tube

The region outside the tube can be treated in a similar fashion. Set

$$Q_{\rm e}=\hat{P}-\hat{A}\frac{K_1(\pi r/L)}{K_1(\pi R/L)}, \quad (3.14)$$

where $K_1(z)$ is the modified Bessel function of the second kind (MacDonald function). Substituting (3.14) in (3.2) we obtain

$$\frac{d^2Q_{\rm e}}{dr^2}+\frac{1}{r}\frac{dQ_{\rm e}}{dr}+\left(\Lambda_{\rm e}^2-\frac{1}{r^2}\right)Q_{\rm e}=F_{\rm e}-\frac{\omega^2 K_1(\pi r/L)}{V_{\rm Ae}^2 K_1(\pi R/L)}\hat{A}. \quad (3.15)$$

The function $Q_{\rm e}$ satisfies the boundary conditions

$$Q_{\rm e}\to 0 \text{ as } r\to\infty, \quad Q_{\rm e}=0 \text{ at } r=R. \quad (3.16)$$

In what follows we impose the condition that $\Im(\Lambda_{\rm e})>0$ when $\Im(\omega)>0$. Then it follows from the asymptotics of the Hankel function of the first kind for $|z|\to\infty$ (Abramowitz and Stegun 1964),

$$H_1^{(1)}(z)\sim\sqrt{\frac{2}{\pi z}}e^{i(z-3\pi/4)} \quad (-\pi<\arg z<2\pi), \quad (3.17)$$

that the solution of the homogeneous equation (3.15) satisfying the first boundary condition in (3.16) can be taken to be equal to $H_1^{(1)}(\Lambda_{\rm e}r)$. We can take the solution satisfying the second boundary condition in (3.16) in the form

$$J_1(\Lambda_{\rm e}R)H_1^{(1)}(\Lambda_{\rm e}r)-J_1(\Lambda_{\rm e}r)H_1^{(1)}(\Lambda_{\rm e}R).$$

Once again using the relation $H_1^{(1)}(z)=J_1(z)+iY_1(z)$ and (3.11), we obtain

$$G_{\rm e}(r,s;\omega)=\frac{i\pi s}{2H_1^{(1)}(\Lambda_{\rm e}R)}\big\{\Theta(s-r)H_1^{(1)}(\Lambda_{\rm e}s)$$
$$\times\big[J_1(\Lambda_{\rm e}R)H_1^{(1)}(\Lambda_{\rm e}r)-J_1(\Lambda_{\rm e}r)H_1^{(1)}(\Lambda_{\rm e}R)\big]+\Theta(r-s)H_1^{(1)}(\Lambda_{\rm e}r)$$
$$\times\big[J_1(\Lambda_{\rm e}R)H_1^{(1)}(\Lambda_{\rm e}s)-J_1(\Lambda_{\rm e}s)H_1^{(1)}(\Lambda_{\rm e}R)\big]\big\}. \quad (3.18)$$

The solution of (3.15) satisfying the boundary conditions (3.16) is given by

$$Q_{\rm e}(r)=\int_R^\infty G_{\rm e}(r,s;\omega)\left\{F_{\rm e}(s)-\frac{\omega^2 K_1(\pi s/L)}{V_{\rm Ae}^2 K_1(\pi R/L)}\hat{A}\right\}ds. \quad (3.19)$$

https://doi.org/10.1017/S0022377805004101 Published online by Cambridge University Press

3.3. Matching solutions

The solutions in the internal and external regions have to satisfy the boundary conditions (3.6) at $r = R$. It follows from (3.7) and (3.14) that $\hat{P}_\mathrm{i} = \hat{P}_\mathrm{e} = \hat{A}$ at $r = R$, so that the first boundary condition in (3.6) is satisfied automatically. Using (3.7) and (3.11)–(3.13) we obtain

$$\left.\frac{d\hat{P}_\mathrm{i}}{dr}\right|_{r=R} = \int_0^R \frac{sJ_1(\Lambda_\mathrm{i}s)}{RJ_1(\Lambda_\mathrm{i}R)}\left\{F_\mathrm{i} - \frac{\omega^2 I_1(\pi s/L)}{V_\mathrm{Ai}^2 I_1(\pi R/L)}\hat{A}\right\} ds + \frac{\pi I_1'(\pi R/L)}{LI_1(\pi R/L)}\hat{A}. \tag{3.20}$$

Using the Bessel and modified Bessel equations, it is straightforward to derive the relation

$$\int_0^R sI_1(\pi s/L)J_1(\Lambda_\mathrm{i}s)\,ds = \frac{RV_\mathrm{Ai}^2}{\omega^2}\left[\frac{\pi}{L}J_1(\Lambda_\mathrm{i}R)I_1'(\pi R/L) - \Lambda_\mathrm{i}J_1'(\Lambda_\mathrm{i}R)I_1(\pi R/L)\right]. \tag{3.21}$$

Using this relation we rewrite (3.20) as

$$\left.\frac{d\hat{P}_\mathrm{i}}{dr}\right|_{r=R} = \int_0^R \frac{sJ_1(\Lambda_\mathrm{i}s)}{RJ_1(\Lambda_\mathrm{i}R)}F_\mathrm{i}(s)\,ds + \frac{\Lambda_\mathrm{i}J_1'(\Lambda_\mathrm{i}R)}{J_1(\Lambda_\mathrm{i}R)}\hat{A}. \tag{3.22}$$

Calculations for the external region parallels those for the internal region. Using (3.1), (3.14), (3.18) and (3.19) we obtain

$$\left.\frac{d\hat{P}_\mathrm{e}}{dr}\right|_{r=R} = -\int_0^\infty \frac{sH_1^{(1)}(\Lambda_\mathrm{e}s)}{RH_1^{(1)}(\Lambda_\mathrm{e}R)}\left\{F_\mathrm{e} - \frac{\omega^2 K_1(\pi s/L)}{V_\mathrm{Ae}^2 K_1(\pi R/L)}\hat{A}\right\} ds + \frac{\pi K_1'(\pi R/L)}{LK_1(\pi R/L)}\hat{A}. \tag{3.23}$$

Also, we may show that

$$\int_R^\infty sK_1(\pi s/L)H_1^{(1)}(\Lambda_\mathrm{e}s)\,ds$$

$$= \frac{RV_\mathrm{Ae}^2}{\omega^2}\left[\Lambda_\mathrm{e}H_1^{(1)'}(\Lambda_\mathrm{e}R)K_1(\pi R/L) - \frac{\pi}{L}H_1^{(1)}(\Lambda_\mathrm{e}R)K_1'(\pi R/L)\right]. \tag{3.24}$$

With the aid of this relation, (3.23) reduces to

$$\left.\frac{d\hat{P}_\mathrm{e}}{dr}\right|_{r=R} = -\int_R^\infty \frac{sH_1^{(1)}(\Lambda_\mathrm{e}s)}{RH_1^{(1)}(\Lambda_\mathrm{e}R)}F_\mathrm{e}(s)\,ds + \frac{\Lambda_\mathrm{e}H_1^{(1)'}(\Lambda_\mathrm{e}R)}{H_1^{(1)}(\Lambda_\mathrm{e}R)}\hat{A}. \tag{3.25}$$

Substituting (3.22) and (3.25) in the boundary condition (3.6) we obtain

$$\hat{A}(\omega) = \frac{T(\omega)}{D(\omega)}, \tag{3.26}$$

where

$$D(\omega) = \Lambda_\mathrm{e}^2\Lambda_\mathrm{i}RJ_1(\Lambda_\mathrm{i}R)H_1^{(1)'}(\Lambda_\mathrm{e}R) - \Lambda_\mathrm{e}^3RJ_1'(\Lambda_\mathrm{i}R)H_1^{(1)}(\Lambda_\mathrm{e}R), \tag{3.27}$$

$$T(\omega) = \Lambda_\mathrm{i}J_1(\Lambda_\mathrm{i}R)\int_R^\infty s\Lambda_\mathrm{e}H_1^{(1)}(\Lambda_\mathrm{e}s)F_\mathrm{e}(s)\,ds$$

$$+ \Lambda_\mathrm{e}^3H_1^{(1)}(\Lambda_\mathrm{e}R)\int_0^R s\Lambda_\mathrm{i}^{-1}J_1(\Lambda_\mathrm{i}s)F_\mathrm{i}(s)\,ds. \tag{3.28}$$

In what follows we also use the expression for $\hat{P}_\mathrm{e}$. With the aid of (3.11), (3.24), the relation obtained from (3.24) by substituting r for R, and the expression for

https://doi.org/10.1017/S0022377805004101 Published online by Cambridge University Press

$\int_R^r sJ_1(\Lambda_e s)K_1(\pi s/L)\,ds$ similar to (3.24), we reduce the expression for $\hat{P}_e$ to

$$\hat{P}_e(r;\omega) = \frac{H_1^{(1)}(\Lambda_e r)}{H_1^{(1)}(\Lambda_e R)}\hat{A}(\omega) + \int_R^\infty G_e(r,s;\omega)F_e(s)\,ds. \tag{3.29}$$

Examining this expression together with (3.26) suggests that $\hat{P}_e(r;\omega)$ has poles at the zeros of $D(\omega)$ and also at the zeros of $H_1^{(1)}(\Lambda_e R)$. However, using (3.11), (3.18) and (3.26)–(3.28) we may rewrite (3.29) as

$$\begin{aligned}\hat{P}_e(r;\omega) = \frac{\Lambda_e H_1^{(1)}(\Lambda_e r)}{D(\omega)}\Bigg\{ &\frac{\pi i}{2}R[\Lambda_i J_1(\Lambda_i R)J_1'(\Lambda_e R) - \Lambda_e J_1(\Lambda_e R)J_1'(\Lambda_i R)] \\ &\times \int_R^\infty s\Lambda_e H_1^{(1)}(\Lambda_e s)F_e(s)\,ds - \Lambda_e^2\int_0^R s\Lambda_i^{-1}J_1(\Lambda_i s)F_i(s)\,ds\Bigg\} \\ &- \frac{\pi i}{2}\Bigg\{J_1(\Lambda_e R)\int_r^\infty sH_1^{(1)}(\Lambda_e s)F_e(s)\,ds \\ &+ H_1^{(1)}(\Lambda_e r)\int_R^r sJ_1(\Lambda_e s)F_e(s)\,ds\Bigg\}.\end{aligned} \tag{3.30}$$

This expression clearly shows that $\hat{P}_e(r;\omega)$ has poles *only* at the zeros of $D(\omega)$; it is regular at the zeros of $H_1^{(1)}(\Lambda_e R)$.

4. Asymptotic solution for large times

We now turn to a study of the asymptotic behaviour of the magnetic pressure perturbation for $t \to \infty$. We start from the asymptotic behaviour of $A(t) = P(t,R)$, and then proceed to the asymptotic behaviour of $P_e(t,r)$ that determines the difference between leaky and non-leaky waves.

In accordance with (3.26), $A(t)$ is given by the inverse Laplace transform

$$A(t) = \frac{1}{2\pi}\int_{i\sigma-\infty}^{i\sigma+\infty}\frac{T(\omega)}{D(\omega)}e^{-i\omega t}\,d\omega, \tag{4.1}$$

where the constant σ is positive but otherwise arbitrary. So far, the functions $D(\omega)$ and $T(\omega)$ are determined only for $\Im(\omega) > 0$. To calculate the asymptotics of $A(t)$ as $t \to \infty$ we need to analytically continue these functions to the lower half of the complex plane.

To reveal the analytical properties of the functions $D(\omega)$ and $T(\omega)$, first note that $J_1(z)$ is an entire function and its power series expansion contains odd powers of z only (Abramowitz and Stegun 1964). This implies that $zJ_1(z)$ and $J_1'(z)$ are entire functions of z^2. Therefore, $\Lambda_i J_1(\Lambda_i R)$ and $J_1'(\Lambda_i R)$ are entire functions of ω. The function $H_1^{(1)}(z)$ can be written in the form

$$H_1^{(1)}(z) = J_1(z) + \frac{2i}{\pi}\left[J_1(z)\ln\frac{z}{2} - \frac{1}{z} + \kappa(z)\right], \tag{4.2}$$

where $\kappa(z)$ is an entire function of z with power series expansion containing odd powers of z only. This implies that the only singularities of the functions $\Lambda_e H_1^{(1)}(\Lambda_e R)$ and $\Lambda_e^2 H_1^{(1)'}(\Lambda_e R)$ are those due to the logarithmic terms proportional

https://doi.org/10.1017/S0022377805004101 Published online by Cambridge University Press

to $\ln\Lambda_e$. On the basis of these results we conclude that the only singularities of $D(\omega)$ and $T(\omega)$ are those related to the terms proportional to $\ln\Lambda_e = \ln[(\omega^2 - \omega_{Ae}^2)/V_{Ae}^2]^{1/2}$, so these singularities are the logarithmic branch points $\omega = \pm\omega_{Ae}$.

To obtain single-valued branches of $D(\omega)$ and $T(\omega)$ we make cuts in the complex ω-plane along the real axis from $-\infty$ to $-\omega_{Ae}$ and from ω_{Ae} to ∞. The function $\omega^2 - \omega_{Ae}^2$ maps the complex ω-plane with these cuts on the complex plane with the cut along the positive real axis. We define the principal sheet of the Riemann surface of $D(\omega)$ and $T(\omega)$ by choosing the branch of the square root that maps this plane on the upper part of the complex plane, and the branch of the logarithm that maps the upper part of the complex plane on the strip $0 < \Im(z) < \pi$. Hence we have $\Im(\Lambda_e) > 0$ and $0 < \Im(\ln\Lambda_e) < \pi$ on the principal sheet.

It is straightforward to see that $\hat{P}_e(r;\omega)$ is also an analytic function of ω on the ω-plane with cuts from $-\infty$ to $-\omega_{Ae}$ and from ω_{Ae} to ∞. The principal sheet of the Riemann surface for $\hat{P}_e(r;\omega)$ is the same as for $D(\omega)$ and $T(\omega)$. Since $\Im(\Lambda_e) > 0$ on the principal sheet, $\hat{P}_e(r;\omega) \to 0$ as $r \to \infty$ on the principal sheet. This fact enables us to also use another name for the principal sheet and call it the physical sheet. In what follows we will term other sheets of the Riemann surface as either non-principal or unphysical.

At this point our analysis splits in two parts. We study the asymptotic behaviour of leaky and non-leaky waves separately.

4.1. Asymptotic behaviour of non-leaky waves

We consider the asymptotic behaviour of waves in the case when $\rho_i > \rho_e$, so that $V_{Ai} < V_{Ae}$. This is the case that typically arises in coronal loops. We restrict our analysis to long waves, i.e. we assume that $L \gg R$. The zeros of $D(\omega)$ on the principal sheet are the eigenfrequencies of the tube oscillations. This inspires us to call $D(\omega)$ the dispersion function. If ω_0 is an eigenfrequency of a static MHD configuration, then ω_0^2 is real (see, e.g., Priest 2000). This means that all zeros of $D(\omega)$ have to be either on the real or on the imaginary axes. Since imaginary zeros of $D(\omega)$ should be in complex conjugate pairs, the existence of imaginary zeros of $D(\omega)$ would imply instability. Since a magnetic tube with straight magnetic field lines is stable, we conclude that all zeros of $D(\omega)$ are real. Since only the interval $(-\omega_{Ae}, \omega_{Ae})$ of the real axis belongs to the principal sheet, it follows that any zero ω_0 of $D(\omega)$ must satisfy the inequality $|\omega_0| < \omega_{Ae}$. Hence, we can assume that $R|\Lambda_{i,e}| \ll 1$ when looking for zeros of $D(\omega)$. Now, using the approximate expressions (Abramowitz and Stegun 1964) valid for $|z| \ll 1$,

$$J_1(z) \approx \frac{z}{2}\left(1 - \frac{z^2}{8}\right), \quad J_1'(z) \approx \frac{1}{2}\left(1 - \frac{3z^2}{8}\right), \tag{4.3a}$$

$$H_1^{(1)}(z) \approx -\frac{2i}{\pi z}\left\{1 - \frac{z^2}{2}\ln\frac{z}{2} + \frac{z^2}{4}(1 - 2E + \pi i)\right\}, \tag{4.3b}$$

$$H_1^{(1)'}(z) \approx \frac{2i}{\pi z^2}\left\{1 + \frac{z^2}{2}\ln\frac{z}{2} + \frac{z^2}{4}(1 + 2E - \pi i)\right\}, \tag{4.3c}$$

where E is the Euler constant, we rewrite the equation $D(\omega) = 0$ in the approximate form as

$$\frac{1}{(R\Lambda_i)^2} + \frac{1}{(R\Lambda_e)^2} = -\ln\frac{R\Lambda_e}{2} - E + \frac{1}{4} + \frac{\pi i}{2}. \tag{4.4}$$

https://doi.org/10.1017/S0022377805004101 Published online by Cambridge University Press

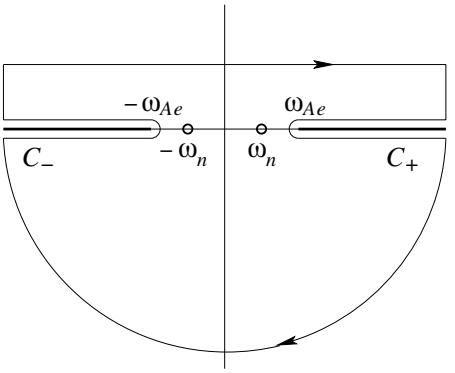

Figure 1. Sketch of the closed integration contour used to evaluate the integral in (4.1). The arrows on the contour show the direction of integration. The thick solid lines show the cuts.

In the first-order approximation we neglect the right-hand side of this equation and obtain $\omega^2 = \omega_k^2$, where ω_k^2 is the square of the kink frequency given by

$$\omega_k^2 = \frac{2\rho\omega_{\rm A}^2}{\rho_{\rm i} + \rho_{\rm e}}, \tag{4.5}$$

where we have used the equilibrium constraint that $\rho_{\rm i}\omega_{\rm Ai}^2 = \rho_{\rm e}\omega_{\rm Ae}^2 = \rho\omega_{\rm A}^2$.

In the next order approximation, we substitute $\omega^2 = \omega_k^2 + \varepsilon$ in the left-hand side and $\omega^2 = \omega_k^2$ in the right-hand side, where $\varepsilon \ll \omega_k^2$. Then, using the relation $\Lambda_{\rm e} \approx ik\Delta$, where

$$k = \frac{\pi}{L}, \quad \Delta = \left|\frac{\rho_{\rm i} - \rho_{\rm e}}{\rho_{\rm i} + \rho_{\rm e}}\right|^{1/2}, \tag{4.6}$$

we obtain

$$\ln\frac{R\Lambda_{\rm e}}{2} \approx \ln\frac{\Delta kR}{2} + \frac{\pi i}{2}. \tag{4.7}$$

With the aid of this relation, we obtain

$$\varepsilon = \frac{1}{2}\omega_k^2\Delta^4(kR)^2\left(\ln\frac{\Delta kR}{2} + E - \frac{1}{4}\right).$$

Hence, we may conclude that, in the long-wavelength approximation, the equation $D(\omega) = 0$ has exactly two roots, $\omega = \pm\omega_m$, where

$$\omega_m \approx \omega_k\left\{1 + \frac{1}{4}\Delta^4(kR)^2\left(\ln\frac{\Delta kR}{2} + E - \frac{1}{4}\right)\right\}. \tag{4.8}$$

This expression coincides with an expression given by Edwin and Roberts (1983).

We see that the function $\hat{A}(\omega)$ is meromorphic on the principal sheet of the Riemann surface with the two simple poles at $\omega = \pm\omega_m$. Now, to calculate the asymptotic behaviour of $A(t)$ as $t \to \infty$, we close the Bromwich integration contour in (4.1) as shown in Fig. 1. It is assumed that the radius of the semi-circle becomes arbitrarily large. Since the contour is traversed in the clockwise direction, which is the negative direction, the contour integral is equal to $-2\pi i$ times the sum of the residues with respect to the poles at $\omega = \pm\omega_m$. The residue with respect to $\omega = \omega_m$

https://doi.org/10.1017/S0022377805004101 Published online by Cambridge University Press

is equal to

$$\lim_{\omega\to\omega_m}\frac{(\omega-\omega_m)T(\omega)}{D(\omega)}e^{-i\omega t}=\chi_m e^{-i\omega_m t}, \tag{4.9}$$

where

$$\chi_m=T(\omega_m)\left(\left.\frac{dD}{d\omega}\right|_{\omega=\omega_m}\right)^{-1}.$$

It is straightforward to show that χ_n is real and the residue with respect to $\omega=-\omega_m$ is equal to $-\chi_m e^{i\omega_m t}$, so that altogether

$$\oint\frac{T(\omega)}{D(\omega)}e^{-i\omega t}\,d\omega=-4\pi\chi_m\sin(\omega_m t). \tag{4.10}$$

Using (3.17) and the asymptotic formula (Abramowitz and Stegun 1964)

$$J_1(z)\sim\sqrt{\frac{2}{\pi z}}\cos(z-3\pi/4)\quad(|\arg z|<\pi), \tag{4.11}$$

valid for $|z|\to\infty$, it is not difficult to show that $T(\omega)/D(\omega)=\mathcal{O}(|\omega|^{-1})$ when $|\omega|\to\infty$. This implies that the integral along the semi-circle, as well as the integrals along the two vertical parts of the closed contour, tend to zero when the radius of the semi-circle tends to infinity. Let us denote by $\mathscr{C}_-$ the contour running from $-\infty$ along the lower side of the left cut, turning around $\omega=-\omega_{\rm Ae}$, and then running back to $-\infty$ along the upper side of the left cut (see Fig. 1). The contour $\mathscr{C}_+$ runs from ∞ along the upper side of the right cut, turns around $\omega=\omega_{\rm Ae}$, and then runs back to ∞ along the lower side of the right cut. The integral over the contour $\mathscr{C}_-$ can be written as

$$\int_{\mathscr{C}_-}\frac{T(\omega)}{D(\omega)}e^{-i\omega t}\,d\omega=\int_{-\infty}^{-\omega_{\rm Ae}}\left\{\frac{T^-(\omega)}{D^-(\omega)}-\frac{T^+(\omega)}{D^+(\omega)}\right\}e^{-i\omega t}\,d\omega,$$

where the superscripts '$-$' and '$+$' indicate the values of a function at the lower and the upper side of the cut, respectively. Integrating by parts and taking into account that $T(\omega)/D(\omega)\to0$ as $|\omega|\to\infty$, and that $T^-(-\omega_{\rm Ae})=T^+(-\omega_{\rm Ae})$ and $D^-(-\omega_{\rm Ae})=D^+(-\omega_{\rm Ae})$, we obtain that

$$\int_{\mathscr{C}_-}\frac{T(\omega)}{D(\omega)}e^{-i\omega t}\,d\omega=\mathcal{O}\left(\frac{1}{\omega_k t}\right)\quad\text{as } t\to\infty. \tag{4.12}$$

The same estimate is valid for the integral over $\mathscr{C}_+$. Hence, eventually we arrive at the asymptotic expression (valid for $t\to\infty$)

$$A(t)\sim-2\chi_m\sin(\omega_m t). \tag{4.13}$$

Let us now study the asymptotic behaviour of $P_{\rm e}(t,r)$. This function is given by

$$P_{\rm e}(t,r)=\frac{1}{2\pi}\int_{i\sigma-\infty}^{i\sigma+\infty}\hat{P}_{\rm e}(r;\omega)e^{-i\omega t}\,d\omega, \tag{4.14}$$

where $\hat{P}_{\rm e}(r;\omega)$ is determined by (3.29) or by (3.30). It is proved in Appendix A that $P_{\rm e}(t,r)=0$ for $r>r_0+V_{\rm Ae}t$; recall that r_0 is chosen by the condition that the plasma is not perturbed for $r>r_0$ at the initial moment of time. This result is not surprising. To clarify its physical nature, consider perturbations with wavelength much smaller than r. Then we can use the WKB approximation and look for solutions of (2.4) proportional to $\exp[i(k_r r-\omega t)]$. As a result, we obtain the dispersion relation

https://doi.org/10.1017/S0022377805004101 Published online by Cambridge University Press

$\omega = V_{\rm Ae}\sqrt{k^2+k_r^2}$ with $k = \pi/L$. Thus, the group velocity $\partial\omega/\partial k_r = V_{\rm Ae}k_r(k^2 + k_r^2)^{-1/2} < V_{\rm Ae}$, so that the energy of perturbations cannot propagate faster than the speed $V_{\rm Ae}$.

The function $\hat{P}_{\rm e}(r;\omega)$ has the same analytical properties and the same Riemann surface as the functions $D(\omega)$ and $T(\omega)$. Hence, for any fixed r, the asymptotic behaviour of $P_{\rm e}(t,r)$ can be evaluated in the same way as for $A(t)$. It is easy to show that the contribution of the second term in (3.29) decays as t^{-1}, and the only non-decaying contribution is given by those poles of the first term that coincide with the zeros of $D(\omega)$. Eventually we obtain that, for any fixed r, the asymptotics of $P_{\rm e}(t,r)$ as $t\to\infty$ is given by

$$P_{\rm e}(t,r) \sim -2\chi_m \sin(\omega_m t)\frac{H_1^{(1)}(\Lambda_{\rm e}r)}{H_1^{(1)}(\Lambda_{\rm e}R)}\bigg|_{\omega=\omega_m}. \tag{4.15}$$

This expression can be simplified if we take $\omega_m \approx \omega_k$ when calculating the last term in (4.15). Then we obtain $\Lambda_{\rm e} \approx ik\Delta$, with Δ given by (4.6). This result together with the relation (Abramowitz and Stegun 1964)

$$H_1^{(1)}(ix) = -\frac{2}{\pi}K_1(x) \quad (x>0) \tag{4.16}$$

enables us to rewrite (4.15) as

$$P_{\rm e}(t,r) \sim -\frac{2\chi_m K_1(kr\Delta)}{K_1(kR\Delta)}\sin(\omega_m t). \tag{4.17}$$

Since $K_1(x) \sim (2x/\pi)^{-1/2}e^{-x}$ for $x\to\infty$, we conclude that $P_{\rm e}(t,r)$ decays exponentially as $r\to\infty$.

If we substitute $P(t,r) = \widetilde{P}(r)e^{-i\omega t}$ in (2.4), we then obtain an eigenvalue problem for $\widetilde{P}(r)$ with ω^2 being the spectral parameter. The solution of this problem has to be regular at $r=0$ and vanish as $r\to\infty$. It also has to satisfy the two boundary conditions (3.6) at $r=R$. It is straightforward to show that ω_m^2 is the eigenvalue with the eigenfunction $\widetilde{P}(r)$ given by $\widetilde{P}(r) = K_1(kr\Delta)$ for $r>R$. This eigenfunction corresponds to the kink mode of the tube oscillations (see Edwin and Roberts 1983). Hence, the spatial behaviour of the asymptotics of $P_{\rm e}(t,r)$ is described by the eigenfunction corresponding to the kink mode. We do not discuss the asymptotic behaviour of $P_{\rm i}(t,r)$ because the main difference between the leaky and non-leaky waves resides in the asymptotic behaviour of $P_{\rm e}(t,r)$. However, it is easy to show that the spatial behaviour of the asymptotics of $P_{\rm i}(t,r)$ is also given by the eigenfunction of the kink mode. Hence, we conclude that the spatial behaviour of the asymptotics of $P(t,r)$, both inside and outside the tube, is given by the eigenfunction of the kink mode.

Using (3.29) it is straightforward to show that $\hat{P}_{\rm e}(r;\omega)$ decays exponentially as $r\to\infty$, and this decay is homogeneous with respect to ω. This implies that $P_{\rm e}(t,r)$ decays exponentially as $r\to\infty$, and this decay is homogeneous with respect to t. Let us denote by $P_{\rm e}^{\rm a}(t,r)$ the asymptotic expression for $P_{\rm e}(t,r)$ as $t\to\infty$, which is the kink mode of the tube (it is given by the right-hand side of (4.17)). $P_{\rm e}^{\rm a}(t,r)$ also decays exponentially as $r\to\infty$, and this decay is homogeneous with respect to t. Let us now take arbitrary $\varepsilon_1 > 0$ and r_1 such that $|P_{\rm e}(t,r)| < \varepsilon_1/2$ and $|P_{\rm e}^{\rm a}(t,r)| < \varepsilon_1/2$ for $r > r_1$ and any t. Then $|P_{\rm e}(t,r) - P_{\rm e}^{\rm a}(t,r)| < \varepsilon_1$ for $r > r_1$ and any t. Now we take t_1 such that $|P_{\rm e}(t,r) - P_{\rm e}^{\rm a}(t,r)| < \varepsilon_1$ for $r \leqslant r_1$ and $t > t_1$. As

https://doi.org/10.1017/S0022377805004101 Published online by Cambridge University Press

a result we obtain that $|P_{\rm e}(t,r) - P_{\rm e}^{\rm a}(t,r)| < \varepsilon_1$ for $t > t_1$ and any r. Hence, the eigenfunction of the kink mode gives the asymptotics of the solution of the initial value problem as $t \to \infty$ which is homogeneous with respect to r.

4.2. Asymptotic behaviour of leaky waves

Consider the asymptotic behaviour of waves in the case when $\rho_{\rm i} < \rho_{\rm e}$, so that $V_{\rm Ai} > V_{\rm Ae}$. Once again we restrict our analysis to long waves. And once again we first study the asymptotic behaviour of $A(t)$, and then the asymptotic behaviour of $P_{\rm e}(t,r)$.

The analytic properties of $D(\omega)$, $T(\omega)$ and $\hat{P}_{\rm e}(r;\omega)$ remain the same as in the case when $V_{\rm Ai} < V_{\rm Ae}$, and so does the principal sheet of the Riemann surface of these functions. The difference arises when we calculate the zeros of $D(\omega)$. If we assume that there are zeros of $D(\omega)$ on the principal sheet, then, as in the previous section, we arrive at the conclusion that they must be in the interval $(-\omega_{\rm Ae}, \omega_{\rm Ae})$. After that, repeating the same calculations, we obtain that, in the first-order approximation, these zeros are equal to $\pm\omega_k$. Since now $\omega_k > \omega_{\rm Ae}$ and the next order approximation gives only small corrections, the zeros cannot be in the interval $(-\omega_{\rm Ae}, \omega_{\rm Ae})$. In addition, in the next order approximation we obtain that these zeros have non-zero imaginary parts which also contradicts the assumption that they are in the interval $(-\omega_{\rm Ae}, \omega_{\rm Ae})$. Hence, we arrive at the conclusion that there are no zeros of $D(\omega)$ on the principal sheet.

Since there are no zeros of $D(\omega)$ on the principal sheet of the Riemann surface, we cannot evaluate the asymptotic behaviour of $A(t)$ by closing the Bromwich integration contour in such a way that the entire closed contour is on the principal sheet of the Riemann surface: a part of the closed contour has to be on one or more non-principal sheets. Here our analysis follows the classical paper by Sedláček (1971) on the electrostatic oscillations in cold inhomogeneous plasmas. However, our analysis is simpler than that by Sedláček because in our case the plasma is homogeneous inside and outside the tube.

As we have already noted, the multivaluedness of the functions $D(\omega)$, $T(\omega)$ and $\hat{P}_{\rm e}(r;\omega)$ is due to $\ln \Lambda_{\rm e} = \frac{1}{2}\ln[(\omega^2 - \omega_{\rm Ae}^2)/V_{\rm Ae}^2]$, so that the Riemann surface of $D(\omega)$, $T(\omega)$ and $\hat{P}_{\rm e}(r;\omega)$ is the same as that of $\ln(\omega^2 - \omega_{\rm Ae}^2)$. The Riemann surface of this function consists of infinitely many copies of the complex ω-plane with the cuts from $-\infty$ to $-\omega_{\rm Ae}$ and from $\omega_{\rm Ae}$ to ∞ properly connected to each other across the cuts. On the principal sheet $0 < \Im[\ln(\omega^2 - \omega_{\rm Ae}^2)] < 2\pi$, and on the other sheets the analytic branches of this function take on values that differ by $2\pi n i$ (for integer n) from the values on the principal sheet. Hence, each sheet can be identified by the value of n with $n = 0$ corresponding to the principal sheet.

Let us now describe how to connect different sheets across the cuts in such a way that the branches of $\ln(\omega^2 - \omega_{\rm Ae}^2)$ on the adjacent sheets are analytic continuations of each other. To do this we examine the boundary values of $\ln(\omega^2 - \omega_{\rm Ae}^2)$ as ω approaches the cuts from the upper or from the lower half-plane. We put $\omega = \tau + i\sigma$, take $\tau < -\omega_{\rm Ae}$ or $\tau > \omega_{\rm Ae}$, and $\sigma \to +0$ or $\sigma \to -0$. As a result we obtain that on the nth sheet of the Riemann surface

$$\lim_{\sigma \to \pm 0} \ln\left(\omega^2 - \omega_{\rm Ae}^2\right) = \ln\left(\tau^2 - \omega_{\rm Ae}^2\right) + \pi i[2n + 1 \mp \operatorname{sgn}(\tau)]. \tag{4.18}$$

Those sides of the corresponding branch cuts on which the boundary values are the same have to be connected. In particular, we have to connect the upper side

https://doi.org/10.1017/S0022377805004101 Published online by Cambridge University Press

of the left cut on the principal sheet ($n = 0$) with the lower side of the left cut on the sheet with $n = 1$, and the lower side of the left cut on the principal sheet with the upper side of the left cut on the sheet with $n = -1$. Similarly, we connect the upper side of the right cut on the principal sheet with the lower side of the right cut on the sheet with $n = -1$, and the lower side of the right cut on the principal sheet with the upper side of the right cut on the sheet with $n = 1$.

We now calculate the zeros of $D(\omega)$ on the sheets with $n = \pm 1$ that satisfy the condition that their imaginary parts tend to zero as $kR \to 0$. The calculation is similar to that which resulted in (4.8), except now

$$\ln(R\Lambda_e) = \ln_0(R\Lambda_e) + \pi n i, \tag{4.19}$$

where $\ln_0(R\Lambda_e)$ indicates the analytic branch of the function $\ln(R\Lambda_e)$ corresponding to the principal sheet, i.e. $0 < \Im[(\ln_0(R\Lambda_e)] < \pi$. Again, we rewrite the equation $D(\omega) = 0$ in the approximate form (4.4). In the first-order approximation we obtain that there are two roots, $\omega = \pm\omega_k$, on every sheet. In the second-order approximation we calculate small corrections to these roots. To do this we have to calculate the right-hand side of (4.4) at $\omega = \omega_0 \equiv \pm\omega_k$. However, ω_0 is just on one of the two cuts of the complex ω-plane. This implies that, in order to calculate $\ln_0(R\Lambda_e)$ we have to prescribe the sign of the imaginary part of the small correction *a priori*. Denoting the small correction as ω_1, then

$$\Im[\ln_0(R\Lambda_e)] \approx \frac{\pi}{2}\{1 - \mathrm{sgn}[\omega_0 \Im(\omega_1)]\}. \tag{4.20}$$

With the aid of this formula we calculate ω_1 and then verify if the sign of $\Im(\omega_1)$ coincides with one prescribed *a priori*. If it does not, then we reject the obtained root $\omega_0 + \omega_1$ as being spurious.

This procedure is straightforward, so that we omit details and present the final result. The two roots on the sheet with $n = 1$ are equal to $\pm\omega_l$, and on the sheet with $n = -1$ they are equal to $\pm\omega_l^*$, where the asterisk indicates a complex conjugate quantity and

$$\omega_l \approx \omega_k \left\{1 + \frac{1}{4}\Delta^4 (kR)^2 \left(\ln\frac{kR\Delta}{2} + E - \frac{1}{4} + \frac{\pi i}{2}\right)\right\}. \tag{4.21}$$

It is worth noting that, if we apply this procedure to the principal sheet ($n = 0$), then the result is that all the roots obtained are spurious. This result is of course consistent with the conclusion that there are no zeros of $D(\omega)$ on the principal sheet.

Now we evaluate the asymptotic behaviour of $A(t)$ using (4.1). To do this we close the Bromwich integration contour as shown in Fig. 2. The closed contour is partly on the principal sheet and partly on the sheets with $n = \pm 1$. The parts of the contour that are either on the principal sheet, or on the sheet with $n = 1$, or on the sheet with $n = -1$ are shown by the solid, dashed and dotted lines, respectively. The radius a of the semi-circle satisfies $a \gg \omega_{Ae}$. The closing part of the contour starts from the point $\omega_1 = a + i\sigma$ and runs vertically downward to the point $\omega_2 = a$. Then it runs through the right cut into the sheet with $n = -1$. In this sheet it runs along the arc with the radius a to the point $\omega_3 \approx \omega_{Ae} + \varepsilon - ia$, where $\varepsilon \ll \omega_{Ae}$ and we have neglected the term of order ω_{Ae} in the expression for the imaginary part of ω_3. After that the contour runs vertically upward to the point $\omega_4 = \omega_{Ae} + \varepsilon$ and returns to the principal sheet through the right cut. On the principal sheet it runs along the semi-circle with radius ε and centre at ω_{Ae} to

https://doi.org/10.1017/S0022377805004101 Published online by Cambridge University Press

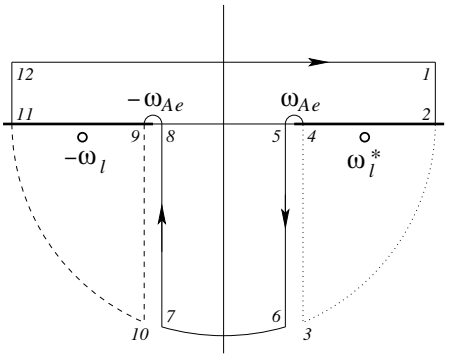

Figure 2. Sketch of the closed integration contour used to evaluate the integral in (3.30). The arrows on the contour show the direction of integration. The thick solid lines show the cuts. The parts of the contour that are either on the principal sheet, or on the sheet with $n = 1$, or on the sheet with $n = -1$ are shown by the solid, dashed and dotted lines, respectively. The numbers $1, \ldots, 12$ indicate the points $\omega_1, \ldots, \omega_{12}$.

the point $\omega_5 = \omega_{\rm Ae} - \varepsilon$, and then vertically downward to the point $\omega_6 \approx \omega_{\rm Ae} - \varepsilon - ia$. From here it runs along the arc of radius a to the point $\omega_7 \approx -\omega_{\rm Ae} + \varepsilon - ia$, then vertically upward to $\omega_8 \approx -\omega_{\rm Ae} + \varepsilon$, and then along the semi-circle with the radius ε and centre at $-\omega_{\rm Ae}$ to $\omega_9 = -\omega_{\rm Ae} - \varepsilon$. At this point the contour runs into the sheet with $n = 1$ through the left cut. At this sheet it runs vertically downward to $\omega_{10} \approx -\omega_{\rm Ae} - \varepsilon - ia$, and then along the arc of radius a to $\omega_{11} = -a$. At this point the contour returns to the principal sheet through the left cut, where it runs vertically upward to $\omega_{12} = -a + i\sigma$. The points $\omega_1, \ldots, \omega_{12}$ are indicated in Fig. 2 by the numbers $1, \ldots, 12$.

It may be noted that the evaluation of the asymptotics of $A(t)$ would be simpler if, instead of cuts shown in Fig. 2, we make one cut from $-\omega_{\rm Ae}$ to $\omega_{\rm Ae}$ (Cally 2005 private communication). In that case the closed integration contour is on the principal sheet of the Riemann surface, although the principal sheet is not a physical sheet in the sense that it is not guaranteed that all the zeros of $D(\omega)$ on this sheet correspond to eigenmodes. Instead, we prefer to use the same cuts employed in the previous section, thus facilitating the comparison of the two cases, $\rho_{\rm i} > \rho_{\rm e}$ and $\rho_{\rm i} < \rho_{\rm e}$.

There are two simple poles on the Riemann surface of the integrand in (3.30) that are inside the closed contour. The first pole is at ω_l^* and it is on the sheet with $n = -1$. The second pole is at $-\omega_l$ and it is on the sheet with $n = 1$. The two poles are shown in Fig. 2 by the small circles. There may be other poles of the integrand inside the closed contour. However, the imaginary parts of these hypothetical poles are not small when $kR \ll 1$. Therefore they give contributions that damp exponentially with a characteristic damping time equal to ω_k^{-1}. Hence, the contributions from the poles at $-\omega_l$ and ω_l^* strongly dominate the contributions from the other poles for $t \gg \omega_k^{-1}$. This enables us to neglect such contributions in what follows.

Since the closed contour is run in the clockwise direction, the contour integral is equal to the sum of the residues with respect to $-\omega_l$ and ω_l^* times $-2\pi i$. The

https://doi.org/10.1017/S0022377805004101 Published online by Cambridge University Press

residue with respect to $\omega = -\omega_l$ is

$$\lim_{\omega \to -\omega_l} \frac{(\omega + \omega_l) T(\omega)}{D(\omega)} e^{-i\omega t} = \chi_l e^{i\omega_l t}, \tag{4.22}$$

where

$$\chi_l = T(-\omega_l) \left(\left. \frac{dD}{d\omega} \right|_{\omega = -\omega_l} \right)^{-1},$$

and the residue with respect to $\omega = \omega_l^*$ is $-\chi_l^* e^{-i\omega_l^* t}$. Hence,

$$\oint \frac{T(\omega)}{D(\omega)} e^{-i\omega t} \, d\omega = 4\pi e^{-\gamma t} \{ \Re(\chi_l) \sin(\omega_m t) + \Im(\chi_l) \cos(\omega_m t) \}, \tag{4.23}$$

where

$$\gamma = \frac{\pi}{8} \omega_k \Delta^4 (kR)^2, \tag{4.24}$$

and $\Re$ indicates the real part of a quantity; we have written $\omega_l = \omega_m + i\gamma$, with ω_m given by (4.8).

Now we take $a \to \infty$ and $\varepsilon \to +0$. Then, in a similar fashion to the previous section, we show that the integrals from ω_1 to ω_3, from ω_6 to ω_7, and from ω_{10} to ω_{12} tend to zero. The integrals from ω_3 to ω_6 and from ω_7 to ω_{10} are of order $(\omega_k t)^{-1}$ when $t \to \infty$. Hence, eventually we obtain

$$A(t) \sim 2e^{-\gamma t} \sin(\omega_m t + \phi) + \mathcal{O}((\omega_k t)^{-1}), \tag{4.25}$$

where $\cos\phi = \Re(\chi_l)$ and $\sin\phi = \Im(\chi_l)$. The second term on the right-hand side of this expression dominates the first term when $t \to \infty$. However, $\gamma/\omega_k = \mathcal{O}(k^2 R^2) \ll 1$. This implies that we can consider the intermediate asymptotics for $\omega_k^{-1} \ll t \lesssim \gamma^{-1}$. For these values of t the first term on the right-hand side of (4.25) dominates the second term. Hence, the intermediate asymptotics of $A(t)$ is given by the first term in (4.25) that describes weakly damped harmonic oscillations of the tube with a frequency $\omega_m \approx \omega_k$.

Let us now study the asymptotic behaviour of $P_{\mathrm{e}}(t, r)$ for large t. The function $P_{\mathrm{e}}(t, r)$ is given by (4.14). Once again it can be evaluated in the same way as the asymptotic behaviour of $A(t)$. Since $0 < \arg(\Lambda_{\mathrm{e}}) < \pi$ on the principal sheet of the Riemann surface, it follows from (4.19) that $-\pi < \arg(\Lambda_{\mathrm{e}}) < 0$ on the sheet with $n = -1$, and $\pi < \arg(\Lambda_{\mathrm{e}}) < 2\pi$ on the sheet with $n = 1$. These inequalities imply that $\Im(\Lambda_{\mathrm{e}}) < 0$ on the sheets with $n = \pm 1$. Then it follows from (3.17) that $H_1^{(1)}(\Lambda_{\mathrm{e}} s)$ is an exponentially growing function of s on these sheets. It seems that this fact causes problems when we try to make the analytic continuation of $\hat{P}_{\mathrm{e}}(r; \omega)$ on the non-principal sheets because (3.30), determining $\hat{P}_{\mathrm{e}}(r; \omega)$, contains improper integrals involving $H_1^{(1)}(\Lambda_{\mathrm{e}} s)$. However this is only an apparent problem because $F_{\mathrm{e}}(s) = 0$ for $r > r_0$.

As in calculating the asymptotic behaviour of $A(t)$, we take into account only the contributions of the poles at $-\omega_l$ and ω_l^*. The integral of $\hat{P}_{\mathrm{e}}(r; \omega)$ over the closed contour is equal to $-2\pi i$ times the sum of the residues of $\hat{P}_{\mathrm{e}}(r; \omega)$ at $-\omega_l$ and ω_l^*. Evaluating the residues (see Appendix B, (B 5) and (B 11)) and taking $\omega_m \approx \omega_k$, we obtain

$$\oint \hat{P}_{\mathrm{e}}(r; \omega) \, e^{-i\omega t} \, d\omega = \frac{4e^{-\gamma t}}{\pi k R \Delta} \Re \{ \chi_l e^{i\omega_k t} H_1^{(1)}(-kr\Delta - i\Gamma r) \}, \tag{4.26}$$

https://doi.org/10.1017/S0022377805004101 Published online by Cambridge University Press

where

$$\Gamma = \frac{\pi}{8R}(1+\Delta^2)(kR\Delta)^3. \tag{4.27}$$

Now we let $\varepsilon \to 0$. As a result the integrals along the contours $4,5$ and $8,9$ vanish. Also, taking $a \to \infty$ we find that the integrals along the contour $6,7$ vanish. On the principal sheet $\hat{P}_{\rm e}(r;\omega)$ decays as $|\omega|^{-1}$ when $|\omega| \to \infty$, so that the integrals along the contours $1,2$ and $11,12$ also vanish as $a \to \infty$. However, the situation with the integrals along the contours $2,3$ and $10,11$ is more complicated. The equations of these contours can be written as $\omega = ae^{-i\varphi}$, where φ varies from 0 to $\pi/2 - \omega_{\rm Ae}/a + \mathcal{O}(\alpha^{-3})$ on the contour $1,2$, and from $\pi/2 + \omega_{\rm Ae}/a + \mathcal{O}(\alpha^{-3})$ to π on the contour $11,12$. For $a \gg \omega_{\rm Ae}$ we obtain $\Lambda_{\rm e}^2 \approx a^2 e^{-2i\varphi}/V_{\rm Ae}^2$. Since $\Im(\Lambda_{\rm e}) > 0$ on the principal sheet, $\Lambda_{\rm e} \approx -ae^{-i\varphi}/V_{\rm Ae}$. Now, taking account of (4.19), we obtain that $\Lambda_{\rm e} \approx ae^{-i\varphi}/V_{\rm Ae}$ on the sheets with $n = \pm 1$, and it follows from (3.17) that $|H_1^{(1)}(\Lambda_{\rm e} r)| \sim (2V_{\rm Ae}/\pi a r)^{1/2} \exp(ar\sin\varphi/V_{\rm Ae})$. Using this result and (3.19) we obtain the estimate

$$|\hat{P}_{\rm e}(r;\omega)e^{-i\omega t}| \sim \text{constant} \times a^{-1/2} \exp[a\sin\varphi(r/V_{\rm Ae} - t)], \tag{4.28}$$

valid as $a \to \infty$ and $0 < \varphi < \pi$. This result implies that the integrals along the contours $2,3$ and $10,11$ vanish as $a \to \infty$ provided $t > r/V_{\rm Ae}$.

Finally, treating the integrals along the contours $3,4$ and $5,6$, and along the contours $7,8$ and $9,10$ in much the same way as for the asymptotics of $A(t)$ (see Sec. 4.2), we obtain that they are of the order of $(\omega_k t)^{-1}$ as $t \to \infty$. Hence, eventually we arrive at the asymptotic expression

$$P_{\rm e}(t,r) \sim \frac{4e^{-\gamma t}}{\pi kR\Delta}\Re\{\chi_l e^{i\omega_k t} H_1^{(1)}(-kr\Delta - i\Gamma r)\} + \mathcal{O}((\omega_k t)^{-1}). \tag{4.29}$$

Once again the first term on the left-hand side of this expression gives only the intermediate asymptotics with $\omega_k^{-1} \ll t \lesssim \gamma^{-1}$. However, t now has also to satisfy the condition $t > r/V_{\rm Ae}$. This condition means that (4.29) gives an asymptotic description which is non-homogeneous with respect to r: the larger r is the larger the values of t for which (4.29) is valid. In fact, the first term on the right-hand side of (4.29) gives the asymptotics of $P_{\rm e}(t,r)$ only for moderate values of r satisfying $r \lesssim V_{\rm Ae}\gamma^{-1}$. When $r \gg V_{\rm Ae}\gamma^{-1}$, the condition $t > r/V_{\rm Ae}$ implies that $t \gg \gamma^{-1}$ and the second term on the right-hand side of (4.29) dominates the first one.

It is instructive to calculate the intermediate asymptotics of $P_{\rm e}(t,r)$ for values of r that are much bigger than the wavelength, i.e. for r satisfying $k^{-1} \ll r < tV_{\rm Ae}$ (note that, since ω_k is of the order of $kV_{\rm Ae}$, the inequality $t \gg \omega_k^{-1}$ implies $tV_{\rm Ae} \gg k^{-1}$). Using (3.17) and (4.29) we obtain

$$P_{\rm e}(t,r) \sim \frac{4\sqrt{2}e^{\Gamma r - \gamma t}}{(\pi\Delta)^{3/2}kR\sqrt{kr}}\Re\{\chi_l \exp[i(\omega_k t - kr\Delta - \pi/4)]\}. \tag{4.30}$$

We see that, at distances from the tube much larger than the wavelength, the perturbation has the form of an exponentially growing harmonic waves propagating from the tube with the phase speed $\omega_k(k\Delta)^{-1}$, though $P_{\rm e}(t,r) = 0$ for $r > tV_{\rm Ae}$. The group speed is equal to the phase speed, so that the energy propagates away from the tube. This is in agreement with the intuitive idea that tube oscillations damp due to energy leakage from the tube.

The right-hand side of (4.29) is a solution of the linear MHD equations called a leaky mode. This solution does not have any physical meaning on its own because

it grows exponentially at infinity. Its physical meaning is provided by the fact that it gives the intermediate asymptotics of the solution of the initial value problem for moderate values of r.

5. Discussion

In the previous section we studied the asymptotics of the solution of the initial value problem describing the kink oscillations of a thin magnetic tube. In the case when $\rho_{\rm i} > \rho_{\rm e}$ ($V_{\rm Ai} < V_{\rm Ae}$) we have shown that the asymptotics of the solution of the initial value problem for kink oscillations is given by a normal mode of the linear ideal MHD equations corresponding to the tube kink oscillations with frequency ω_k. This normal mode decays exponentially as $r \to \infty$ and gives asymptotics for $t \to \infty$ that is homogeneous with respect to r.

In the case when $\rho_{\rm i} < \rho_{\rm e}$ ($V_{\rm Ai} > V_{\rm Ae}$) the asymptotics of the solution of the initial value problem is given by a leaky mode of the linear ideal MHD. The leaky mode describes a damped kink oscillation with frequency ω_k. It exponentially grows as $r \to \infty$. Therefore it has no physical meaning on its own. Its physical meaning exists only due to the fact that it describes the asymptotic state of the solution of the initial value problem. The leaky mode describes only an intermediate asymptotics valid for $\omega_k^{-1} \ll t \lesssim \gamma^{-1}$, where γ is the decrement of the leaky mode. In addition, the asymptotics is non-homogeneous with respect to r and valid only for $r < tV_{\rm Ae}$.

Recently, Cally (2003) has argued that there are leaky modes even in the case when $\rho_{\rm i} > \rho_{\rm e}$. To understand what kind of solution of the linear MHD equations is considered a leaky mode by Cally, we have to look for the zeros of the dispersion function $D(\omega)$ on non-principal sheets of the Riemann surface. In fact, it is instructive to start from the case where $\rho_{\rm i} < \rho_{\rm e}$. In what follows we consider only zeros of $D(\omega)$ that are close to the real axis in the complex ω-plane, i.e. the zeros with the imaginary part much smaller than the real part. In Sec. 4.2 we found that there are two such roots on each of the sheets with $n = 1$ and $n = -1$. Repeating the same procedure we easily find that there are two roots given by $\omega = \pm\omega_n = \pm[\omega_m + (2n-1)i\gamma]$ on the sheet with $n = 1, 2, \ldots$, and two roots given by $\omega = \pm\omega_n = \pm[\omega_m + (2n+1)i\gamma]$ on the sheet with $n = -1, -2, \ldots$. In particular, these formulae reproduce the results obtained in Sec. 4.2 for $n = \pm 1$: $\pm\omega_1 = \pm\omega_l$, $\pm\omega_{-1} = \pm\omega_l^*$. We can always obtain a solution of the linear MHD equations with all variables proportional to $e^{\mp\omega_n t}$. In particular, in such a solution

$$P_{\rm e}(t,r) = P_n^{\pm}(t,r) = \text{constant} \times e^{\mp i\omega_n t} H_1^{(1)}(\Lambda_{\rm e} r). \tag{5.1}$$

At large distances from the tube ($kr \gg 1$) the functions $P_n^{\pm}(t,r)$ have the form of propagating harmonic waves with the amplitude slowly varying both in space and in time. The wave propagates either toward the tube or outward. If the wave propagates toward the tube then there is an energy flux toward the tube from infinity. It is generally agreed that such solutions are unphysical. If the wave propagates outward then it is said that the corresponding solution satisfies the radiation condition. Usually such a solution is considered as physically meaningful and is called a 'leaky mode'. However, we prefer to call it an 'improper mode'. The reason for this will be made clear in what follows.

In Sec. 4.2 we have shown that the solutions corresponding to $\omega = -\omega_1 = -\omega_l$ on the sheet with $n = 1$ and $\omega = \omega_{-1} = \omega_l^*$ on the sheet with $n = -1$ satisfy the radiation condition. To find out if there are zeros of $D(\omega)$ on the sheets with

https://doi.org/10.1017/S0022377805004101 Published online by Cambridge University Press

$n \neq \pm 1$ that satisfy the radiation condition, we have to study the asymptotics of $H_1^{(1)}(\Lambda_e r)$ on these sheets for $kr \gg 1$. The asymptotics of $H_1^{(1)}(\Lambda_e r)$ on the sheets with $n = -1, 0, 1$ has already been calculated with the aid of (3.17). To calculate the asymptotics on the other sheets we use the relation that follows from (4.2) and is valid for any integer m,

$$H_1^{(1)}(ze^{2\pi m i}) = H_1^{(1)}(z) - 4mJ_1(z). \tag{5.2}$$

Then, using (3.17) and (4.11) it is straightforward to obtain that the asymptotic behaviour of $H_1^{(1)}(z)$ as $|z| \to \infty$ is given by

$$H_1^{(1)}(z) \sim \begin{cases} (2m-1)\sqrt{\dfrac{2}{\pi z}}\, e^{i(z+\pi m+\pi/4)}, & \pi(2m-1) < \arg z < 2\pi m, \\ 2m\sqrt{\dfrac{2}{\pi z}}\, e^{-i(z+\pi m+\pi/4)}, & 2\pi m < \arg z < \pi(2m+1), \end{cases} \tag{5.3}$$

where $m = \pm 1, \pm 2, \dots$. With the aid of (5.3) we can show that $P_n^+(t,r)$ with $n > 0$ and $P_n^-(t,r)$ with $n < 0$ do not satisfy the radiation condition. On the other hand, we obtain for $kr \gg 1$ that

$$P_n^-(t,r) \propto r^{-1/2} \exp[(2n-1)(\Gamma r - \gamma t)] \exp[i(\omega_k t - k\Delta r)] \quad (n = 1, 2, \dots), \tag{5.4}$$

$$P_n^+(t,r) \propto r^{-1/2} \exp[(2n+1)(\gamma t - \Gamma r)] \exp[i(k\Delta r - \omega_k t)] \quad (n = -1, -2, \dots). \tag{5.5}$$

Hence, $P_n^-(t,r)$ with $n > 0$ and $P_n^+(t,r)$ with $n < 0$ satisfy the radiation condition and can be called improper modes. Their amplitudes decay exponentially with time and grow exponentially with distance from the tube. An improper mode is defined with accuracy up to a multiplicative complex constant. It can be shown that the multiplicative constants can be chosen such that $P_{-n}^+(t,r) = [P_n^-(t,r)]^*$, for $n = 1, 2, \dots$. This implies that we can restrict our analysis to the improper modes $P_n^-(t,r)$ $(n = 1, 2, \dots)$ only and call $P_n^-(t,r)$ the nth improper mode. We have already pointed out that the first improper mode, $P_1^-(t,r)$, has no physical meaning on its own because it grows exponentially with distance from the tube. Its significance is related to the fact that it describes the intermediate asymptotics of the solution of the initial value problem. The other improper modes also grow exponentially with distance from the tube, so that they are also physically meaningless on their own. Also, in contrast to the first improper mode, they are not related to the solution of the initial value problem at all. Hence, we conclude that the improper modes starting from the second one are unphysical and should be eliminated from consideration. The only improper mode that is physically meaningful is the first one, and the name 'leaky mode' applies to this mode only.

Consider the case where $\rho_i > \rho_e$. Repeating the calculation carried out in Sec. 4.1 and using (4.19) we immediately obtain that there are two zeros of $D(\omega)$ on the nth sheet given by $\omega = \pm\omega_n = \pm(\omega_m + 2in\gamma)$. When $n = 0$ this reproduces the result obtained in Sec. 4.1. Using this result, the fact that $\Im(\Lambda_e) > 0$ on the principal sheet and (4.19), we obtain that, on the nth sheet, Λ_e is given by

$$\Lambda_e \approx (-1)^n (ik\Delta + n\Upsilon), \tag{5.6}$$

https://doi.org/10.1017/S0022377805004101 Published online by Cambridge University Press

where $\Upsilon = \frac{1}{4}\pi(1-\Delta^2)R^2(k\Delta)^3$. Let us once again consider the solutions of the linear MHD equations with all variables proportional to $e^{\mp i\omega_n t}$. The perturbation of the magnetic pressure outside the tube is given in these solutions by (5.1). Using (5.3) and (5.6), and taking $\omega_m \approx \omega_k$ we obtain that, for $kr \gg 1$,

$$P_{\rm e}(t,r) = P_n^{\pm}(t,r) \propto r^{-1/2}\exp(k\Delta r \pm 2n\gamma t)\exp[i(\mp\omega_k t - n\Upsilon r)]. \qquad (5.7)$$

In contrast to the case where $\rho_{\rm i} < \rho_{\rm e}$ this expression does not have the form of a harmonic wave with the amplitude slowly varying in space because $k\Delta \gg \Upsilon$. However, in spite of this, Cally (2003) suggested considering such a solution as satisfying the radiation condition if the last multiplier on the right-hand side of (5.7) describes an outgoing wave. Let us accept Cally's suggestion and once again call a solution satisfying the radiation condition an improper mode. Then we immediately conclude that $P_n^+(t,r)$ is an improper mode if $n < 0$ and $P_n^-(t,r)$ is an improper mode if $n > 0$. Note that the improper modes decay exponentially with time.

As with the case $\rho_{\rm i} < \rho_{\rm e}$, the improper modes have no physical meaning on their own because they grow exponentially with distance from the tube. Also, all improper modes are not related to the solution of the initial value problem because, in accordance with Sec. 4.1, the asymptotic behaviour of the solution of the initial value problem is described by the normal mode. Hence, in the case where $\rho_{\rm i} > \rho_{\rm e}$ all improper modes are unphysical and therefore should not be considered as leaky modes.

What Cally (2003) found and called a 'leaky mode' is, in fact, the improper mode $P_{-1}^+(t,r)$ with complex frequency $\omega_m - 2i\gamma$. We obtain this frequency from Cally's equation (8) if we take the cold plasma limit of his equation and impose the condition that the imaginary part of the frequency has to be negative. We would like to emphasize once again that none of these modes is physically meaningful.

6. Summary and conclusions

In this paper we studied kink oscillation of thin magnetic tubes in a cold plasma. The normal modes of kink oscillations exist only when the plasma density $\rho_{\rm i}$ in the tube is bigger than the plasma density $\rho_{\rm e}$ outside the tube ($\rho_{\rm i} > \rho_{\rm e}$). This is the usual circumstance in coronal loops. Using the Laplace transform we solved the initial value problem for kink oscillations and then studied the asymptotic behaviour of the solution for large times. We found that, when $\rho_{\rm i} > \rho_{\rm e}$, this asymptotic behaviour is described by the normal mode. The normal mode gives asymptotics that is homogeneous with respect to the spatial coordinate r. The frequency of the normal mode is real and it is given by the zero of the dispersion function $D(\omega)$ on the principal sheet of the Riemann surface of this function. The dispersion function $D(\omega)$ is an infinitely valued function and its Riemann surface consists of infinitely many sheets.

In the case where $\rho_{\rm i} < \rho_{\rm e}$, corresponding to a low-density magnetic flux tube, the asymptotic behaviour of the solution of the initial value problem is given by the leaky mode of kink oscillations. The frequency of the leaky mode is determined by the zero of the dispersion function $D(\omega)$ on the first non-principal sheet of the Riemann surface of the dispersion function. It has a negative imaginary part, describing the damping of kink oscillations due to energy leakage. The leaky mode gives only intermediate asymptotics of the solution of the initial value problem, valid for times much bigger than the period of kink oscillation but smaller than (or

https://doi.org/10.1017/S0022377805004101 Published online by Cambridge University Press

of the order of) the characteristic damping time. Additionally, it gives asymptotics that is inhomogeneous with respect to r.

An important property of the leaky mode is that it satisfies the so-called radiation condition. This means that, at large distances from the tube, the leaky mode has the form of an outgoing harmonic wave with an amplitude that is slowly varying in space and time. Also, the leaky mode grows exponentially with the distance from the tube axis, so that it has no physical meaning on its own. Its significance is related to the fact that it gives intermediate asymptotics of the solution of the initial value problem.

When $\rho_{\rm i} < \rho_{\rm e}$, there are infinitely many solutions of the linear MHD equations satisfying the radiation condition. Their frequencies are given by the zeros of $D(\omega)$ on the non-principal sheets of its Riemann surface. We call any solution satisfying the radiation condition an 'improper mode', so that the leaky mode describing the asymptotics of the solution of the initial value problem can also be called an improper mode. All improper modes grow exponentially with the distance from the tube, so they have no physical meaning on their own. In contrast to the first improper mode, also called a leaky mode, all improper modes starting from the second one are not related to the solution of the initial value problem; this fact inspires us to conclude that they are physically meaningless.

We also studied the solutions of the linear MHD equations with frequencies given by the zeros of $D(\omega)$ on the non-principal sheet, in the case when $\rho_{\rm i} > \rho_{\rm e}$. We used a generalization of the radiation condition suggested by Cally (2003) and found that there are infinitely many solutions satisfying the generalized radiation condition. We call these solutions improper modes. Again, all improper modes grow exponentially with distance from the tube. But, in contrast to the case when $\rho_{\rm i} < \rho_{\rm e}$, now none of the improper modes is related to the solution of the initial value problem. Hence we concluded that when $\rho_{\rm i} < \rho_{\rm e}$ all improper modes are physically meaningless solutions of the linear MHD equations.

Our final conclusion is that for the case $\rho_{\rm i} > \rho_{\rm e}$ only the normal mode of kink oscillations arises and there are no leaky modes. In the case when $\rho_{\rm i} < \rho_{\rm e}$ there is exactly one leaky mode of kink oscillations. We can apply these results to the damping of kink oscillations of coronal magnetic loops. Since the plasma density inside a loop is bigger than the density of the surrounding plasma, the kink oscillations of coronal magnetic loops are non-leaky and the damping of these oscillations cannot be related to wave energy leakage in a direction transverse to the loop. Other mechanisms causing decay must be sought if we are to explain the observed damping of kink loop oscillations.

Acknowledgement

The authors are grateful to Professor Paul Cally and Dr Jaume Terradas for constructive comments on a draft of our work. MSR thanks the School of Mathematics and Statistics at the University of St Andrews for warm hospitality while this work was in progress.

Appendix A

In this Appendix we show that $P_{\rm e}(t,r) \equiv 0$ when $r > r_0 + V_{\rm Ae}t$. Using (3.18) and (3.26)–(3.28) we rewrite the expression (3.29) for $\hat{P}_{\rm e}(r;\omega)$ as

$$\hat{P}_{\rm e}(r;\omega) = \hat{P}_{\rm e}^{(1)}(r;\omega) + \hat{P}_{\rm e}^{(2)}(r;\omega) + \hat{P}_{\rm e}^{(3)}(r;\omega), \tag{A 1}$$

https://doi.org/10.1017/S0022377805004101 Published online by Cambridge University Press

where

$$\hat{P}_{\rm e}^{(1)}(r;\omega) = -\frac{\pi i}{2}\left\{ J_1(\Lambda_{\rm e} r)\int_r^\infty s H_1^{(1)}(\Lambda_{\rm e} s) F_{\rm e}(s)\, ds \right.$$
$$\left. + H_1^{(1)}(\Lambda_{\rm e} r)\int_R^r s J_1(\Lambda_{\rm e} s) F_{\rm e}(s)\, ds \right\}, \tag{A 2}$$

$$\hat{P}_{\rm e}^{(2)}(r;\omega) = \frac{\Lambda_{\rm e}^3 H_1^{(1)}(\Lambda_{\rm e} r)}{\Lambda_{\rm i} D(\omega)}\int_0^R s J_1(\Lambda_{\rm i} s) F_{\rm i}(s)\, ds, \tag{A 3}$$

$$\hat{P}_{\rm e}^{(3)}(r;\omega) = \frac{\pi i R \Lambda_{\rm e}^2}{2D(\omega)} H_1^{(1)}(\Lambda_{\rm e} r)\{\Lambda_{\rm i} J_1(\Lambda_{\rm i} r) J_1'(\Lambda_{\rm e} r)$$
$$- \Lambda_{\rm e} J_1(\Lambda_{\rm e} r) J_1'(\Lambda_{\rm i} r)\}\int_R^\infty s H_1^{(1)}(\Lambda_{\rm e} s) F_{\rm e}(s)\, ds. \tag{A 4}$$

Since we consider $r > r_0 + V_{\rm Ae} t$, and $F_{\rm e}(r) = 0$ for $r > r_0$, it follows that the first integral in (A 2) is zero, and we can substitute r_0 for the upper limit of integration in the second integral. Then, changing the order of integration, we obtain

$$P_{\rm e}^{(1)}(t,r) = \frac{1}{2\pi}\int_{i\sigma-\infty}^{i\sigma+\infty} \hat{P}_{\rm e}^{(1)}(r;\omega)\, e^{-i\omega t}\, d\omega$$
$$= -\frac{i}{4}\int_R^{r_0} s F_{\rm e}(s)\, ds \int_{i\sigma-\infty}^{i\sigma+\infty} J_1(\Lambda_{\rm e} s) H_1^{(1)}(\Lambda_{\rm e} r)\, e^{-i\omega t}\, d\omega. \tag{A 5}$$

Since this expression is valid for any $\sigma > 0$, we can take $\sigma \to \infty$, which implies that $|\omega| \to \infty$. Then $\Lambda_{\rm e} \sim \omega/V_{\rm Ae}$ and, using the asymptotic formulae (3.17) and (4.11) we arrive at the asymptotic relation

$$J_1(\Lambda_{\rm e} s) H_1^{(1)}(\Lambda_{\rm e} r) e^{-i\omega t} \sim \frac{2V_{\rm Ae}}{\pi\omega\sqrt{rs}} \exp[i\omega(r - s - V_{\rm Ae} t)/V_{\rm Ae}], \tag{A 6}$$

valid for $|\omega| \to \infty$, $\Im(\omega) > 0$. It follows from (A 6) that the integrand in the integral with respect to ω in (A 5) tends to zero homogeneously with respect to s and $\Re(\omega)$ when $\sigma \to \infty$ and $r - s - V_{\rm Ae} t >$ constant > 0, where $\Re$ indicates the real part of a quantity. Since $s \leqslant r_0$, the latter condition is satisfied if we take $r > r_0 + V_{\rm Ae} t + \epsilon$, where $\epsilon > 0$ and otherwise it is arbitrary. Then we conclude that $P_{\rm e}^{(1)}(t,r) = 0$ for any r satisfying this inequality. Since ϵ is arbitrary, we eventually conclude that $P_{\rm e}^{(1)}(t,r) = 0$ for any $r > r_0 + V_{\rm Ae} t$.

In a similar way we can prove that $P_{\rm e}^{(2)}(t,r) = P_{\rm e}^{(3)}(t,r) = 0$ and, eventually, $P_{\rm e}(t,r) = 0$ for $r > r_0 + V_{\rm Ae} t$.

Appendix B

In this Appendix we calculate the residues of $\hat{P}(r;\omega)e^{-i\omega t}$ at $-\omega_l$ and ω_l^*. We use the expression (3.29) for $\hat{P}(r;\omega)$. Since the second term on the right-hand side of this expression is regular at $\omega = -\omega_l$ and $\omega = \omega_l^*$, the only contribution is given by the first term. Then, using (4.22), we obtain

$$\operatorname*{res}_{\omega=-\omega_l} \hat{P}(r;\omega) e^{-i\omega t} = \chi_l e^{i\omega_l t} \left.\frac{H_1^{(1)}(\Lambda_{\rm e} r)}{H_1^{(1)}(\Lambda_{\rm e} R)}\right|_{\omega=-\omega_l}. \tag{B 1}$$

https://doi.org/10.1017/S0022377805004101 Published online by Cambridge University Press

Since $\omega_l = \omega_m + i\gamma$ with $\gamma \ll \omega_m$ it follows that, at $\omega = \omega_l$,

$$\ln_0(R\Lambda_e) \approx \ln_0(R\Lambda_e)|_{\gamma=0} + \gamma\left(\frac{1}{2\Lambda_e^2}\frac{d\Lambda_e^2}{d\gamma}\right)_{\gamma=0} = \ln_0|R\Lambda_e||_{\gamma=0} + \frac{i\omega_m\gamma}{\omega_m^2 - \omega_{Ae}^2}. \quad (B\,2)$$

When deriving this expression we have used (4.20). Then, recalling that $-\omega_l$ is on the sheet with $n = 1$, using (4.19) and taking $\omega_m \approx \omega_k$, we eventually arrive at

$$\Lambda_e \approx -k\Delta - i\Gamma, \quad (B\,3)$$

where $\Gamma = \frac{1}{8}\pi R^2(1+\Delta^2)(k\Delta)^3$. Note that $\Gamma \ll k\Delta$. Recalling that $kR \ll 1$ and using (4.3) yields

$$H_1^{(1)}(\Lambda_e R) \approx H_1^{(1)}(-kR\Delta) \approx \frac{2i}{\pi kR\Delta}. \quad (B\,4)$$

Substituting (B 3) and (B 4) in (B 1) we obtain

$$\operatorname*{res}_{\omega=-\omega_l} \hat{P}(r;\omega)e^{-i\omega t} \approx \frac{2i\chi_l e^{i\omega_l t}}{\pi kR\Delta} H_1^{(1)}(-kr\Delta - i\Gamma r). \quad (B\,5)$$

The residue at ω_l^* is given by

$$\operatorname*{res}_{\omega=\omega_l^*} \hat{P}(r;\omega)e^{-i\omega t} = -\chi_l^* e^{-i\omega_l^* t}\left.\frac{H_1^{(1)}(\Lambda_e r)}{H_1^{(1)}(\Lambda_e R)}\right|_{\omega=\omega_l^*}. \quad (B\,6)$$

Once again using (4.20) we obtain

$$\ln_0(R\Lambda_e) \approx \ln_0|R\Lambda_e||_{\gamma=0} + \pi i - \frac{i\omega_m\gamma}{\omega_m^2 - \omega_{Ae}^2}. \quad (B\,7)$$

Recalling that ω_l^* is on the sheet with $n = -1$, using (4.19) and taking $\omega_m \approx \omega_k$ yields

$$\Lambda_e \approx k\Delta - i\Gamma. \quad (B\,8)$$

Then, substituting (B 8) in (B 6) and using the approximate expression similar to (B 4), we obtain

$$\operatorname*{res}_{\omega=\omega_l^*} \hat{P}(r;\omega)e^{-i\omega t} \approx \frac{2i\chi_l^* e^{-i\omega_l^* t}}{\pi kR\Delta} H_1^{(1)}(kr\Delta - i\Gamma r). \quad (B\,9)$$

Using (4.2), (4.19), (B 2) and (B 7), it is straightforward to show that

$$H_1^{(1)}(kr\Delta - i\Gamma r) = [H_1^{(1)}(-kr\Delta - i\Gamma r)]^*. \quad (B\,10)$$

It follows from (B 5), (B 9) and (B 10) that

$$\operatorname*{res}_{\omega=\omega_l^*} \hat{P}(r;\omega)e^{-i\omega t} = -\left[\operatorname*{res}_{\omega=-\omega_l} \hat{P}(r;\omega)e^{-i\omega t}\right]^*. \quad (B\,11)$$

References

Abramowitz, M. and Stegun, A. 1964 *Handbook of Mathematical Functions*. New York: Wiley.

Aschwanden, M. J. 2004 *Physics of the Solar Corona*. Berlin: Springer.

Aschwanden, M. J., Fletcher, L., Schrijver, C. J. and Alexander, D. 1999 Coronal loop oscillations observed with the Transition region and Coronal explorer. *Astrophys. J.* **520**, 880–894.

https://doi.org/10.1017/S0022377805004101 Published online by Cambridge University Press

Aschwanden, M. J., Schrijver, C. J., De Pontieu, B. and Title, A. M. 2002 Transverse oscillations in coronal loops observed with TRACE—II. Measurements of geometric and physical parameters. *Solar Phys.* **206**, 99–132.

Cally, P. S. 1986 Leaky and non-leaky oscillations in magnetic-flux tubes. *Solar Phys.* **103**, 277–298.

Cally, P. S. 2003 Coronal leaky tube waves and oscillations observed with trace. *Solar Phys.* **217**, 95–108.

Edwin, P. M. and Roberts, B. 1983 Wave propagation in a magnetic cylinder. *Solar Phys.* **88**, 179–191.

Goossens, M., Andries, J. and Aschwanden, M. J. 2002 Coronal loop oscillations—an interpretation in terms of resonant absorption of quasi-mode kink oscillations. *Astron. Astrophys.* **394**, L39–L42.

Meerson, B. I., Sasarov, P. V. and Stepanov, A. V. 1978 Pulsations of type IV solar radio emission—the bounce-resonance effects. *Solar Phys.* **58**, 165–179.

Nakariakov, V. M. and Ofman, L. 2001 Determination of the coronal magnetic field by coronal loop oscillations. *Astron. Astrophys.* **372**, L53–L56.

Nakariakov, V. M. and Verwichte, E. 2005 Coronal waves and oscillations. *Living Reviews in Solar Phys.* **2**, 3–65.

Nakariakov, V. M., Ofman, L., Deluca, E. E., Roberts, B. and Davila, J. M. 1999 TRACE observation of damped coronal loop oscillations: Implications for coronal heating. *Science* **285**, 862–864.

Priest, E. R. 2000 *Solar Magnetohydrodynamics*. Dordrecht: Reidel.

Roberts, B. 2000 Waves and oscillations in the corona (Invited review). *Solar Phys.* **193**, 139–152.

Roberts, B. 2002 Waves and oscillations in the solar corona: theory. *Solar Variability: From Core to Outer Frontiers*, ESA SP-506, pp. 481–489.

Roberts, B. 2004 MHD waves in the solar atmosphere. *Waves, Oscillations and Small-Scale Transient Events in the Solar Atmosphere: a Joint View from SOHO and TRACE*, SOHO13, ESA SP-547, pp. 1–14.

Roberts, B., Edwin, P. M. and Benz, A. O. 1984 On coronal oscillations. *Astrophys. J.* **279**, 857–865.

Roberts, B. and Nakariakov, V. M. 2003 Theory of MHD waves in the solar corona. *Turbulence, Waves and Instabilities in the Solar Plasma* (ed. R. Erdélyi, K. Petrovay, B. Roberts and M. J. Aschwanden), *NATO Advanced Research Workshop*, Vol. 124. Dordrecht: Kluwer, pp. 167–191.

Ruderman, M. S. and Roberts, B. 2002 Damping of coronal loop oscillations. *Astrophys. J.* **577**, 475–486.

Schrijver, C. J., Aschwanden, M. J. and Title, A. M. 2002 Transverse oscillations in coronal loops observed with TRACE—I. An overview of events, movies, and a discussion of common properties and required conditions. *Solar Phys.* **206**, 69–98.

Schrijver, C. J. and Brown, D. S. 2000 Oscillations in the magnetic field of the solar corona in response to flares near the photosphere. *Astrophys. J.* **537**, L69–L72.

Sedláček, Z. 1971 Electrostatic oscillations in cold inhomogeneous plasma. I. Differential equation approach. *J. Plasma Phys.* **5**, 239–263.

Spruit, H. C. 1982 Propagation speeds and acoustic damping of waves in magnetic-flux tubes. *Solar Phys.* **75**, 3–17.

Verwichte, E., Nakariakov, V. M., Ofman, L. and DeLuca, E. E. 2004 Characteristics of transverse oscillations in a coronal loop arcade. *Solar Phys.* **223**, 77–94.

Wang, T. J. 2004 Coronal loop oscillations: overview of recent results in observations. *Waves, Oscillations and Small-Scale Transient Events in the Solar Atmosphere: a Joint View from SOHO and TRACE*, SOHO13, ESA SP-547, pp. 417–426.

Wang, T. J. and Solanki, S. K. 2004 Vertical oscillations of a coronal loop observed by TRACE. *Astron. Astrophys.* **421**, L33–L36.